International Journal of Antimicrobial Agents 23 (2004) 273–285

INTERNATIONAL JOURNAL OF Antimicrobial Agents

www.ischemo.org

Selective in vitro effects of the farnesyl pyrophosphate synthase inhibitor risedronate on *Trypanosoma cruzi*

Luciana R. Garzoni [a], Aura Caldera [b], Maria de Nazareth L. Meirelles [a], Solange L. de Castro [a], Roberto Docampo [c], Gary A. Meints [d], Eric Oldfield [d], Julio A. Urbina [b,*]

[a] *Departmento de Ultra-estrutura e Biologia Celular, Instituto Oswaldo Cruz, Av. Brasil, 4365, Manguinhos, 21045-900 Rio de Janeiro, RJ, Brazil*

[b] *Laboratorio de Química Biológica, Centro de Biofísica y Bioquímica, Instituto Venezolano de Investigaciones Cientificas, Apartado Postal 21.827, Caracas 1020A, Venezuela*

[c] *Laboratory of Molecular Parasitology, Department of Pathobiology and Center for Zoonoses Research, University of Illinois at Urbana-Champaign, Urbana, IL 61802, USA*

[d] *Department of Chemistry and Department of Biophysics, University of Illinois at Urbana-Champaign, Urbana, IL 61801, USA*

Received 21 March 2003; accepted 3 July 2003

Abstract

We present the results of the first detailed study of the molecular and cellular basis of the antiproliferative effects of the bisphosphonate risedronate (Ris) on *Trypanosoma cruzi*, the causative agent of Chagas' disease. Ris and related compounds, which block poly-isoprenoid biosynthesis at the level of farnesyl pyrophosphate synthase, are currently used for the treatment of bone resorption disorders, but also display selective activity against trypanosomatid and apicomplexan parasites. Ris induced a dose-dependent effect on growth of the extracellular epimastigote form of *T. cruzi*; complete growth arrest and cell lysis ensued at 150 μM. Growth inhibition was associated with depletion of the parasite's endogenous sterols, but complete growth arrest and loss of cell viability took place before full depletion of these compounds, suggesting that disappearance of other essential poly-isoprenoids is involved in its anti-parasitic action. Ris had a variety of effects on cellular ultrastructure, including mitochondrial swelling, disorganisation of other organelles, such as reservosomes and the kinetoplast, together with the appearance of autophagic vesicles and progressive vacuolization of the cytoplasm. Ris had selective antiproliferative effects against the clinically relevant amastigote form of *T. cruzi*, and at 100 μM, was able to prevent completely the development of *T. cruzi* infection of murine muscle heart or Vero cells, and to cure cultures which were already infected. Ris induced drastic ultrastructural alterations in the intracellular parasites and blocked amastigote to trypomastigote differentiation, with no biochemical or ultrastructural effects on the host cells, which fully recovered their normal structure and activity after treatment. Ris is, therefore, a promising lead compound for the development of new drugs against *T. cruzi*.

Keywords: Risedronate; *T. cruzi*; Chagas' disease; Antiproliferative effect; Amastigote

1. Introduction

Chagas disease, caused by *Trypanosoma cruzi*, is endemic in Latin America, affecting 16–18 million people [1]. Transmission occurs mainly by insect vectors (Reduviidae), but also by blood transfusion and congenital routes [2]. Treatment still relies on the use of nifurtimox and benznidazole, drugs that were introduced empirically in the 1970s. However, both these nitroheterocycles frequently produce toxic side effects, have considerable variability in cure rates (depending of the geographic region), and very limited efficacy for treatment of chronic patients. Moreover, the commercial production of nifurtimox has been discontinued since the 1980s in Brazil and more recently in Argentina, Chile and Uruguay. There is, therefore, clearly an unmet need for new, specific chemotherapeutic approaches for the treatment of this serious condition [3,4].

Recent developments in understanding the biochemistry of *T. cruzi* have permitted the identification of several new drug targets in this parasite. Among the most promising

* Corresponding author. Tel.: +58-212-5041479; fax: +58-212-5041093.
E-mail address: jaurbina@ivic.ve (J.A. Urbina).

0924-8579/$ – see front matter © 2003 Elsevier B.V. and the International Society of Chemotherapy. All rights reserved.
doi:10.1016/j.ijantimicag.2003.07.020

are the de novo sterol and phosphatidylcholine biosynthesis pathways, the essential cathepsin L-like protease cruzipain and the unique Kinetoplastida enzymes trypanothione reductase and trypanothione synthase [5,6]. Another promising approach developed recently is interference with the metabolism of inorganic pyrophosphate and various isoprenoid pyrophosphates, which are precursors of several essential cellular components. Both theoretical and experimental work has shown that the antiproliferative effects of nitrogen containing bisphosphonates (NBPs) in vertebrate and plant cells and in the slime mould *Dictyostelium discoideum*, result from a blockade of isoprenoid synthesis at the level of farnesyl pyrophosphate synthase (FFPS, refs. [7–12]). A gene encoding the farnesyl pyrophosphate synthase of *T. cruzi* has been cloned and sequenced and its expression in *Escherichia coli* produced an enzyme which was potently inhibited by NBPs, risedronate (Ris) being among the most active compounds investigated [13].

The selective action of NBPs against trypanosomatid and apicomplexan parasites could result from preferential drug accumulation in the parasite's acidocalcisomes, acidic organelles which contain most of the cell's polyphosphates, complexed with divalent cations such as Ca^{2+} and Mg^{2+} [14,15]. The presence of polyphosphate-rich acidocalcisomes, as well as the recent discovery of several pyrophosphate-utilizing enzymes in trypanosomatids, therefore opens up a potential new route for the treatment of numerous parasitic diseases including Chagas' disease [15–20]. Moreover, since Ris is currently used for the prevention and treatment of postmenopausal and corticosteroid-induced osteoporosis [21], there is extensive data available on its pharmacology, toxicology and tolerance in humans, reducing the costs of development of this drug against Chagas' and other parasitic diseases.

Although the selective antiparasitic activity of bisphosphonates has been demonstrated previously, little information exists on their cellular and molecular basis of action. Here, we present the first detailed study of the effects of Ris on the viability and proliferation of epimastigotes and intracellular amastigotes of *T. cruzi*. Biochemical and ultrastructural alterations induced by the bisphosphonate in both forms of the parasite, as well as in primary cultures of mouse heart muscle and cultured Vero cells, have been investigated using gas–liquid chromatography coupled to mass spectrometry, together with electron and fluorescence microscopy, to obtain a detailed picture of the drug action.

2. Materials and methods

2.1. Parasites

Both the Y [22] and EP [23] strains of *T. cruzi* were used in this work, with essentially identical results. Epimastigotes were grown in liver-infusion (LIT) medium [23] at 28 °C, with strong aeration. Trypomastigote forms of the Y strain were obtained from the supernatant of infected heart muscle cells (10:1 parasites:host cells) grown in complete Eagle medium supplemented with 5% foetal calf serum (FCS), 1 mM $CaCl_2$, 15% horse serum, 1 mM L-glutamine, 2% chick embryo extract, 1000 U/ml penicillin and 50 μg/ml streptomycin (DMEM). After 96 h of infection the parasites were collected by centrifugation then resuspended in DMEM. Handling of live *T. cruzi* was performed according to established guidelines [24].

2.2. Mammalian cell cultures

Hearts of 18-day-old Swiss mouse embryos were submitted to mechanical and enzymatic dissociation using 0.05% trypsin plus 0.01% collagenase in PBS at 37 °C, following the method described previously [25]. The ventricular heart muscle cells (HMCs) were plated on 0.02% gelatin-coated plastic bottles, on glass coverslips in 24-well plates or in Petri dishes. Cells were maintained at 37 °C in a 5% CO_2 atmosphere in DMEM. After 72 h of plating, the cultures were used for the experiments with Ris. Vero cells were maintained in minimal essential medium supplemented with 2% FCS, as described previously [26].

2.3. Effect of risedronate on epimastigotes

Y strain epimastigotes were resuspended in LIT medium at a density of 1×10^7 cells/ml in 24-well plates [27] and 500 μl of the suspension was added to the same volume of Ris solution, previously prepared in LIT at twice the desired final concentration. After 1–8 days of incubation at 28 °C, parasites were counted in a haemocytometer. The motility and morphology of the parasites was monitored by optical microscopy (Axioplan, Zeiss, Oberköchen, Germany). For the EP strain, Ris was added to cultures in conical flasks at a cell density of $0.5–1 \times 10^7$ epimastigotes/ml and followed for 7–10 days. Cell densities were measured by turbidimetry as well as by direct counting in a haemocytometer. Cell viability was followed by trypan blue exclusion, using light microscopy. After the incubation period, cells were harvested by centrifugation and processed for lipid analysis, as described below.

2.4. Effect of risedronate on lipid composition of epimastigotes and Vero cells

For the analysis of the effects of Ris on sterol composition of epimastigotes or Vero cells, total lipids from control and drug-treated cells were extracted, then fractionated into neutral and polar lipid fractions, by using silicic acid column chromatography and gas–liquid chromatography [28–31]. The neutral lipid fraction was first analysed by thin layer chromatography (Merck 5721 silica gel plates; heptane-isopropyl ether–glacial acetic acid [60:40:4] as developing solvent) and by gas–liquid chromatography (isothermal separation on a 4 m glass column packed with 3% OV-1 on

Chromosorb, 100/200 mesh, with nitrogen (24 ml/min) as carrier gas and using flame ionisation detection, on a Varian 3700 gas chromatograph). For structural assignments and quantitative analysis, the neutral lipids were separated by using a high resolution capillary column (25 m × 0.20 mm i.d., Ultra-2 column, 5% phenyl-methyl-siloxane, 0.33 μm film thickness) on a Hewlett-Packard 6890 Plus gas chromatograph equipped with an HP5973A mass sensitive detector. Lipids were injected as chloroform solutions and the column kept at 50 °C for 1 min, then the temperature was increased to 270 °C at a rate of 25 °C/min, and finally to 300 °C, at a rate of 1 °C/min. The carrier gas (He) flow was kept constant at 0.5 ml/min. Injector temperature was 250 °C and the detector was kept at 280 °C. The polar lipid fraction (containing mostly phospholipids) was analysed as described previously [32]. Briefly, the lipid fractions eluting from the silicic acid column with chloroform:methanol (1:1, v/v) were pooled, then further fractionated by thin-layer chromatography on Merck 5721 silica gel plates, using chloroform:methanol:32.5% ammonia w/v (17:7:1; v/v/v) as developing solvent [33]. The phospholipid spots were visualised by using iodine, scraped off, then the total organic phosphorus was measured by using the method of Ames and Dubin [34].

2.5. Effects of risedronate on the proliferation and differentiation of T. cruzi amastigotes in heart muscle and Vero cells

HMCs (1.5×10^5 cells/well in 24-well plates) were infected with culture-derived trypomastigotes (10:1 parasites:host cells), in a final volume of 300 μl DMEM. After 2 h, the cultures were washed with PBS to remove non-adherent parasites and maintained in DMEM. Treatment was performed by following two protocols: (i) addition of 50–200 μM Ris in DMEM immediately after the interaction step; (ii) addition of 100 μM Ris after 48 h of infection. The total volume in each well was 500 μl. At specific times, coverslips (in triplicate) were collected, fixed with Bouin and stained in Giemsa solution. The percentage of infection was quantified by counting randomly at least 300 cells. In addition, the supernatant was collected and counted in a haemocytometer, to obtain the number of released trypomastigotes from the HMCs. The coverslips were used for the fluorescence assays. For electron microscopic analysis, experiments were performed in Petri dishes, maintaining both the number of HMCs/area and proportion of parasites/HMC, then using the two treatment protocols described above.

Vero cells were infected with culture-derived trypomastigotes (10:1 parasites:host cell) for 2 h, then washed three times with PBS to remove non-adherent parasites. Fresh medium, with or without Ris, was then added and the cells incubated for 96 h, with a medium change at 48 h. Quantitation of the number of infected cells was then carried out as described previously [30,31].

2.6. Ultrastructural studies

At chosen times, epimastigotes or infected HMC cells were fixed (60 min/4 °C) with 2.5% glutaraldehyde, 2.5 mM $CaCl_2$ and 0.1 M Na-cacodylate buffer (pH 7.2). After post-fixation for 1 h in cacodylate buffer solution containing 1% OsO_4, 0.8% potassium ferricyanide and 2.5 mM $CaCl_2$, samples were dehydrated in acetone then embedded in Polybed 812 resin. Thin sections (Leica Ultracuts, UCT, Vienna, Austria) were stained with uranyl acetate and lead citrate, and were examined by transmission electron microscopy using an Zeiss EM10C microscope.

2.7. Effect of risedronate on HMC cytoskeletal actin

Using protocol (i), after 144 h of treatment with 100 μM Ris, coverslips containing treated cells were fixed in 4% paraformaldehyde in PBS and stained for 30 min at 37 °C with 4 μg/ml rhodamine-labelled phalloidin in PBS, to stain actin filaments. During the last 5 min, DAPI was added to stain DNA, as described previously [35]. The cultures were observed by using a fluorescence microscope (Axioplan, Zeiss).

2.8. Flow cytometry

Epimastigotes were treated with 50–200 μM Ris in LIT medium at 28 °C. After 4 and 8 days, 500 μl of the cultures were taken and added to the same volume of a solution containing 20 μg/ml propidium iodide, for 30 min. Samples were kept on ice until analysis, which was carried out using a flow cytometer (FACSCalibur, BectonDickinson, San Jose, USA) equipped with Cell Quest and WinMDI2.8 software (Joseph Trotter, Scripps Research Institute, San Diego, USA).

2.9. Statistical analysis

Mean value comparisons were performed by using the Student *t*-test or Anova and Krunskal–Wallis test. *P*-values below 0.05 were considered significant. IC_{50} values were calculated from dose-response curves by using a non-linear regression analysis with the GraFit software package.

2.10. Materials

Risedronate (2-(3-pyridyl)-1-hydroxy-ethane-1,1-bisphosphonate, monosodium salt) was synthesized basically as described previously [12]. Elemental analysis and ^1H, ^{13}C and ^{31}P NMR spectra indicated that the compound was 98.8% pure. Stock solutions were prepared in phosphate buffered saline (PBS) (pH adjusted to 7.4) and sterilized by using a 0.2 μM filter (Millipore). Trypsin and rhodamine-labelled phalloidin were purchased from Sigma Chemical Co. (St. Louis, MO, USA), collagenase was from Aldrich–Sigma

(St. Louis, MO, USA). All other reagents were of analytical grade.

3. Results

3.1. Effects of risedronate on T. cruzi epimastigotes

Ris inhibited in a dose-dependent manner the proliferation of Y strain *T. cruzi* epimastigotes in the range 25–400 μM (Fig. 1), having an $IC_{50} = 30.3 \pm 3.3$ μM ($n = 3$). Against the EP strain (Fig. 2), the activity was similar, with an IC_{50} of 26.4 ± 5.4 μM ($n = 3$). At concentrations 150 μM, Ris induced complete growth arrest and cell lysis of both strains. Growth inhibition was correlated with a dose-dependent reduction of the ratio of endogenous (ergosterol, 24-ethyl-cholesta-5,7,22-trien-3-β-ol and precursors) to exogenous (cholesterol) sterols, and the IC_{50} for this effect was 65.4 ± 3.5 μM (Fig. 2 and Table 1).

T. cruzi epimastigotes contain characteristic membrane-bound organelles called reservosomes, which are terminal vesicles of the cell's endocytic pathway and have a protein-rich matrix, together with lipid droplets [36]. Reservosomes were among the first organelles altered by treatment with Ris (Fig. 3). While reservosomes in control cells showed a typical electron dense matrix (Fig. 3A), treatment with Ris (50 μM, 96 h) led to a marked reduction in the electron density of these organelles (Fig. 3B). In addition to the effects seen in reservosomes, the kinetoplast, a massive arrangement of mitochondrial DNA characteristic of trypanosomatids and related protozoa, was also affected by treatment with Ris. In control cells, this structure consists of a tightly packed row of fibres in a typical 'bar' form (Fig. 3A); however, Ris-treated cells display an irregular compaction of the mitochondrial DNA (Fig. 3B). With higher doses and/or with longer incubation periods, the alterations in these two organelles were intensified (Fig. 3C–F): in cells exposed to Ris at 100 μM for 96 h or 50 μM for 192 h, the reservosomes showed increased degradation of the protein matrix and an abnormal accumulation of lipid inclusions (Fig. 3C and E). Other ultrastructural alterations were also observed in Ris-treated parasites, such as swelling of the mitochondrion with loss of inner membrane and matrix electron density, formation of autophagic vesicles and progressive vacuolization of the cytoplasm (Fig. 3D and F). It was also found, using phase contrast microscopy, that all Ris concentrations which affected cell growth induced rounding of the parasite body and a marked decrease in motility. However, it is interesting to note that in cells treated with up to 200 μM Ris for 192 h, no ultrastructural modifications were detected at the plasma membrane or in the subpellicular microtubules, despite the drastic alterations seen in the intracellular organelles (Fig. 3G). The functional intactness of the plasma membrane in Ris-treated cells was confirmed, using flow cytometry analysis, by the lack of labelling of the drug-treated parasites with propidium iodide (PI), a non-permeant fluorescent dye [37] (data not shown).

3.2. Effect of risedronate on intracellular T. cruzi amastigotes and host cells

Using two different treatment protocols, Ris caused a strong inhibition of the infection of HMCs (Fig. 4). When the drug was added immediately after infection (2 h), a

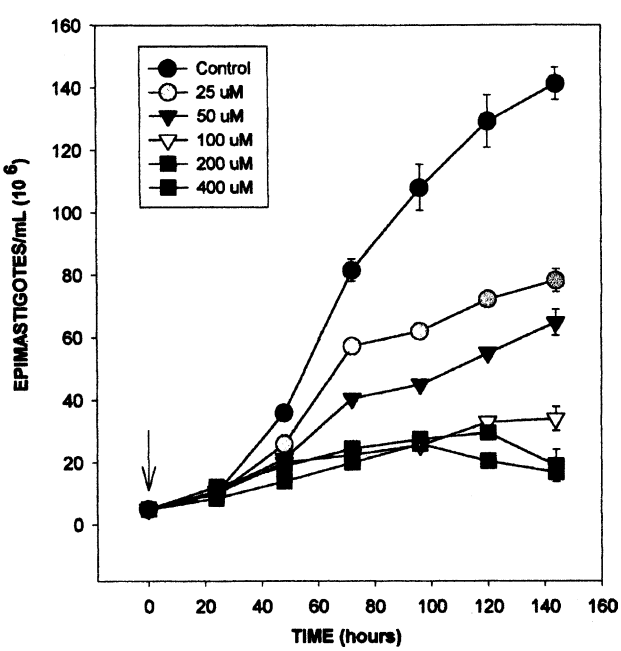

Fig. 1. Effects of risedronate on the proliferation of *T. cruzi* epimastigotes, Y strain. Epimastigotes were cultured in LIT medium at 28 °C, with agitation, as described in Section 2. The graph shows the mean and one standard deviation of duplicates of one representative experiment of four independent experiments.

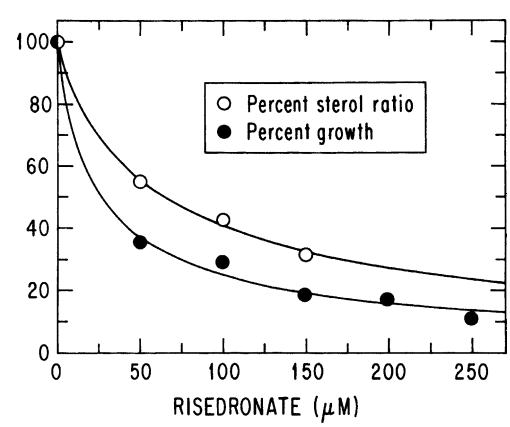

Fig. 2. Effects of risedronate on the proliferation and sterol composition of *T. cruzi* epimastigotes, EP strain. The percent ratio of endogenous to exogenous sterols (open symbols) and the percent growth (closed symbols) after 120 h of incubation with the indicated concentration of the drug are plotted. Experimental details are given in Section 2, Table 1 and caption to Fig. 1. Percent growth is defined as: % growth $= ((N_F - N_I/N_I)_T/(N_F - N_I/N_I)_C) \times 100$, where N_F and N_I are the final and initial cell densities, while T and C refer to treated and control (untreated) cells.

Table 1
Effects of risedronate on the free sterol composition of *Trypanosoma cruzi* epimastigotes (EP stock)[a]

Name	Structure	Ris0 μM	Ris50 μM	Ris100 μM	Ris 150 μM
Exogenous					
Cholesterol	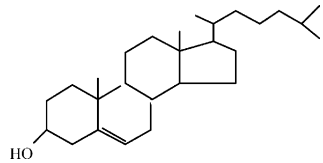	33.9	48.2	54.8	62.1
Endogenous					
24-Methyl-5,7,22-cholesta-trien-3β-ol (ergosterol)	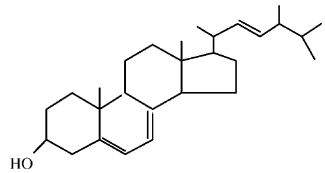	22.5	20.8	20.2	17.3
24-Ethyl-5,7,22-cholesta-trien-3β-ol	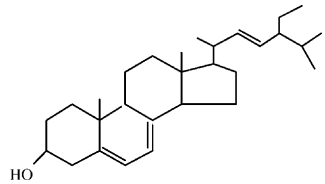	16.0	22.8	25.0	20.6
Ergosta-5,7-dien-3β-ol	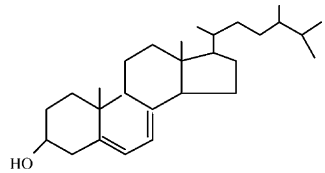	9.6	3.2	n.d.	n.d.
Ergosta-5,7,24(24^1)-dien-3β-ol	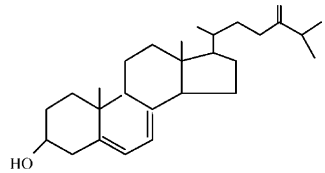	13.9	5.0	n.d.	n.d.
Ergosta-7,24(24^1)-dien-3β-ol	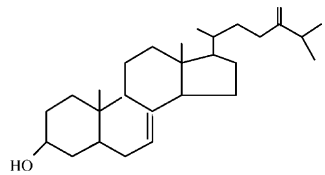	4.1	n.d.	n.d.	n.d.
Endogenous/exogenous sterols		1.95	1.07	0.82	0.61

[a] Sterols were extracted from *T. cruzi* epimastigotes cultured in LIT medium and drugs added at a cell density of 5×10^6 epimastigotes/ml; they were separated from polar lipids by silicic acid column chromatography and analyzed by quantitative capillary gas–liquid chromatography and mass spectrometry. Results are expressed as mass percent.

dose-dependent reduction in the percentage of infected cells was seen as a function of time. The inhibition was statistically significant for treatment with 200 μM after 72 h, with 100 and 150 μM Ris after 96 h and with 50 μM Ris, after 120 h (Fig. 4A). No infected cells were observed with Ris at 200, 150 and 100 μM after 96, 120 and 144 h, respectively. Under our experimental conditions, Ris did not interfere with the contractility of either infected or uninfected HMCs.

Addition of 100 μM Ris 48 h after infection also led to a highly significant reduction in the percentage of infected cells, 72 to 144 h after treatment. With the longer exposure, the infection disappeared completely (Fig. 4B). We also investigated the effects of Ris on the release of trypomastigotes from infected cells in this model, after completion of the intracellular cycle of the parasite. In control HMC cultures, the first two peaks of trypomastigote release to the supernatant occurred at 96 h and 192 h post-infection (Fig. 4C). Treatment with 100 μM Ris, starting 48 h post-infection, significantly inhibited (61.1%) such release after 48 h of treatment (96 h post-infection), while after 96 and 144 h of treat-

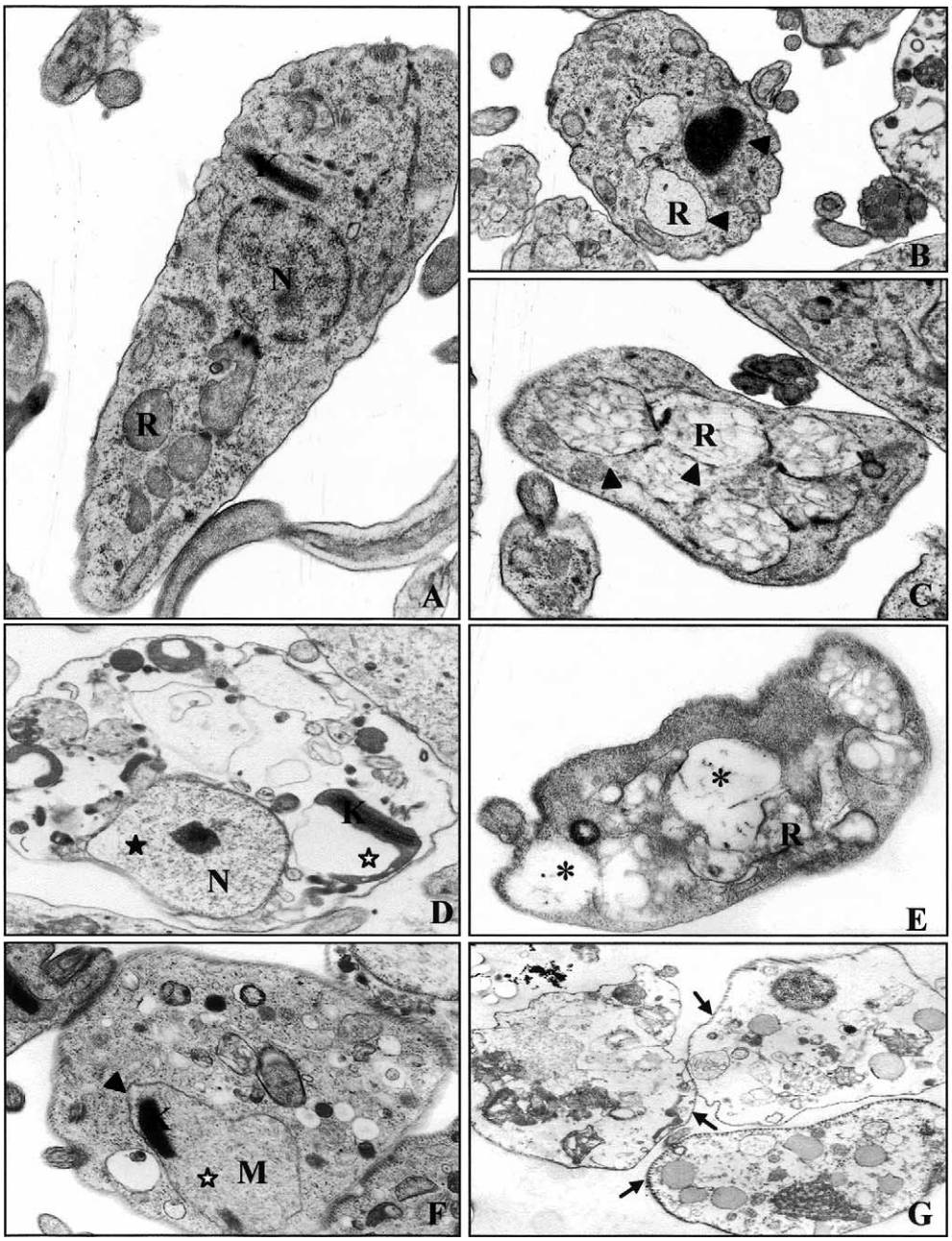

Fig. 3. Effects of risedronate on the ultrastructure of *T. cruzi* epimastigotes (Y strain). (A) Control parasite showing organelles with their characteristic aspect, such as kinetoplast (k), reservosomes (R) and nucleus (N). (B) 50 μM Ris for 96 h led to alterations on the kinetoplast and reservosomes (arrow heads). (C, D) 100 μM Ris for 96 h caused (C) marked alterations of reservosomes (arrow heads) and (D) alterations in the nucleus (dark star), strong cytoplasmic vacuolisation, together with mitochondrial swelling (white star); (E) 50 μM Ris for 192 h led to the appearance of autophagic vesicles in the parasite, besides intense vacuolisation (asterisks), and loss of proteic matrix in reservosomes; (F) 100 μM Ris for 192 h led to mitochondrial swelling (white star) and alterations on the kinetoplast (arrow head); (G) 200 μM Ris for 192 h caused breakdown of internal organelles, but plasma membrane and subpellicular microtubules were preserved (arrows). Magnifications: (A) 15,300×; (B) 11,500×; (C) 18,000×; (D) 14,600×; (E) 23,500×; (F) 6300×.

ment, no trypomastigotes were detected in the supernatant (Fig. 4C).

A quantitative analysis of the effects of Ris (added immediately after infection) on the percentage of infected host cells, intracellular parasite load and host cell viability, was carried out after 96 h of incubation (Fig. 5). The IC_{50} was 66.0 ± 0.8 μM for Y strain in HMC cells and 30.1 ± 0.6 μM for the EP strain, in Vero cells; the minimal concentration required to completely eradicate the infection in these experimental models, were 150 and 100 μM Ris, respectively. At higher concentrations, there was a slight, non-statistically significant reduction in the total number of host cells, but no alteration of their gross morphology. No effects on the sterol (cholesterol) or phospholipid composition of uninfected Vero cells were detected after incubation with 100 μM Ris for 96 h (data not shown). Infected Vero cells

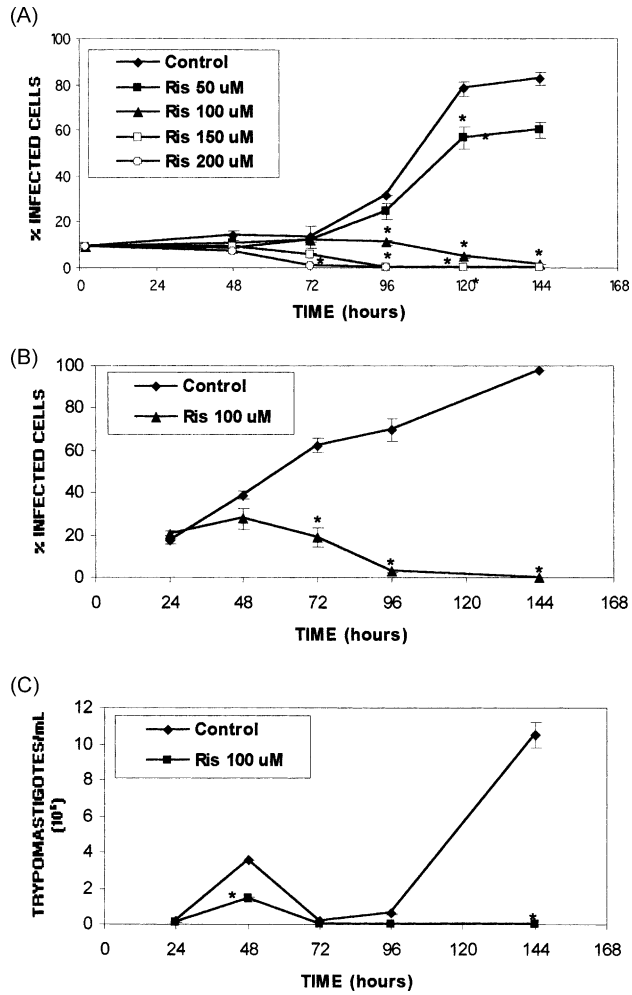

Fig. 4. Time and concentration dependence of the effects of risedronate on the infection of HMC by *T. cruzi*. (A) Ris (50–200 μM) added to the cultures after 2 h of infection and the percentage of infected cells followed as a function of time. (B, C) Ris (100 μM) added to the cultures after 48 h of infection induced (B) a potent inhibitory effect on infection of HMC and (C) on trypomastigote release. Asterisks indicate statistical differences in relation to control cultures. The graphs show the mean and standard deviation of triplicates of one representative experiment of four independent experiments.

treated with Ris at concentrations that eradicated the infection had no relapse of the infection after further incubation in a drug-free medium, indicating a trypanocidal effect.

Using optical microscopy, we followed the morphological alterations induced by Ris on intracellular amastigotes (Fig. 6). After 72 h of treatment with 100 μM Ris, the parasites began to exhibit morphological alterations with progressive damage. Treatment with Ris inhibited the differentiation to trypomastigotes (see also Fig. 4C) and, after 120–144 h of treatment, essentially no intact intracellular parasites were observed. Changes induced by drug treatment were also investigated at the ultrastructural level in both parasites and host cells, using electron microscopy. It was found that in untreated HMC cells after 144 h of infection, intracellular parasites (mainly trypomastigotes) exhibited normal morphology, with characteristic empty spaces, devoid of electron density, in cytoplasmic regions close to parasite cells (Fig. 7B). Treatment with 100 μM Ris for 96 h (144 h of infection) caused marked alteration of the overall shape of the parasites, together with swelling of the sarcoplasmic reticulum of the HMCs (Fig. 7C). The potent effect of Ris on intracellular amastigotes can be seen in Fig. 7D. These parasites exhibited mitochondrial swelling, the presence of autophagic vesicles and intense vacuolisation, as seen with the extracellular epimastigotes. No intact parasites could be seen with 100 μM Ris after 144 h of treatment (192 h of infection). At this point, HMCs exhibited myofibrils with Z lines as well as mitochondrial, sarcoplasmic reticulum and cytoplasmic structures very similar to those seen in the control cultures (compare Fig. 7A and E). All of these findings clearly indicate that Ris induces the destruction of parasite cells, but permits the recovery of normal structure and metabolism of host cells, together with de novo protein biosynthesis. This notion is reinforced by the presence of a large number of ribosomes in the sarcoplasmic reticulum (Fig. 7E). To explore further these observations, we investigated the distribution of actin filaments in HMCs, labelling the cells with rhodamine-phalloidin and DAPI. Control HMCs showed highly developed actin-containing myofibrils (Fig. 8A). Infection with *T. cruzi* for 144 h led to a breakdown of actin filaments close to the intracellular parasites (Fig. 8C). However, after treatment of infected HMCs with 100 μm Ris for 142 h, the host cells presented both polygonal and filamentous configurations of actin (Fig. 8E), and no parasites (small blue dots) were detected using DAPI (Fig. 8D and F).

4. Discussion

Ris induced a dose-dependent effect on the ratio of endogenous/exogenous epimastigote sterols, consistent with a blockade of the synthesis of these essential components at a pre-squalene level (Fig. 2 and Table 1), in agreement with the accepted primary target of NBPs in eukaryotic cells, FPPS [7–12]. However, although this effect was associated with a reduction in parasite growth rate, the antiproliferative effects were observed at drug concentrations significantly lower than those required to produce equivalent effects on the sterol composition of the cells (Figs. 1 and 2 and Table 1). This may be explained by the fact that blockade at the level of FPPS depletes the cells of other essential poly-isoprenoids. Similar conclusions have been reached in a previous study, which investigated the combined effects of risedronate and ketoconazole at fixed concentrations on epimastigotes [16].

One of the characteristic ultrastructural effects of sterol biosynthesis inhibitors on trypanosomatid parasites is a marked swelling of their single, giant mitochondrion, which correlates with depletion of the endogenous parasite sterols and leads to cell lysis [38–43]. Previous work from our

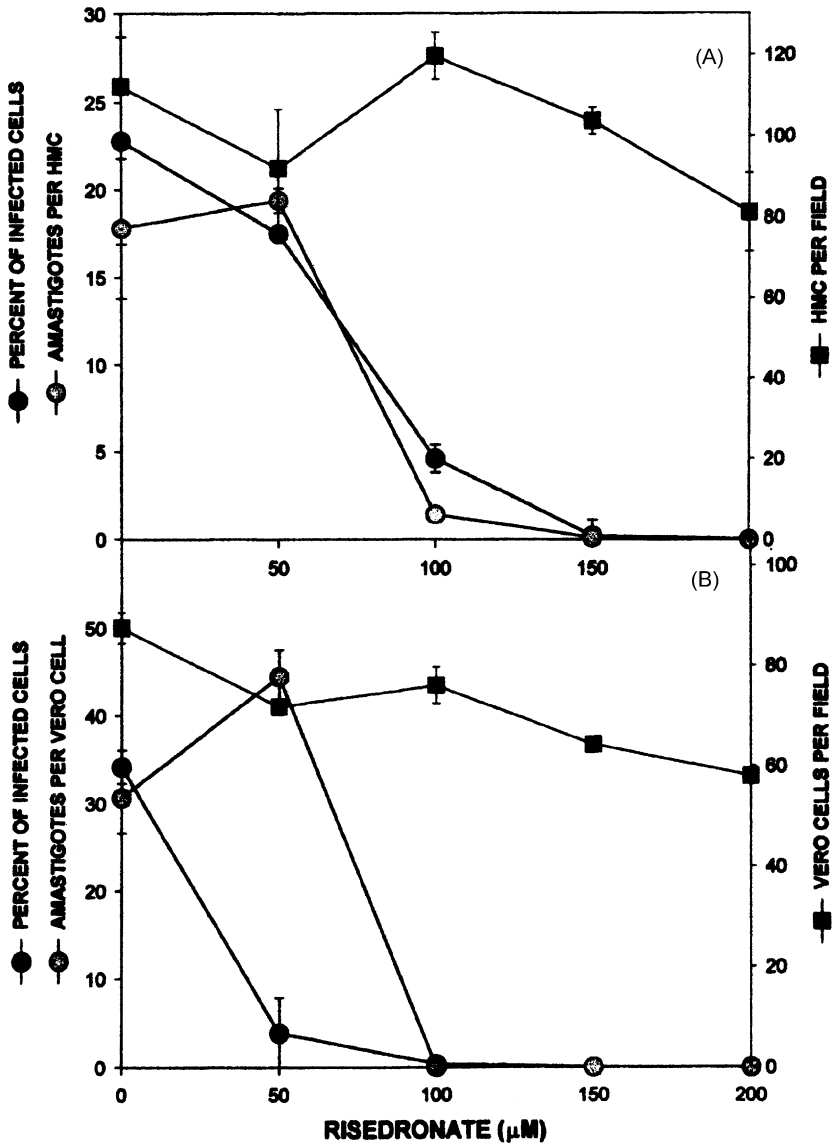

Fig. 5. Concentration dependence of the effects of risedronate on the proliferation of *T. cruzi* amastigotes in mammalian cells. Shown are the percentage of infected cells (●), the number of amastigotes per cell (○) and the number of host cells per field (■) after 96 h of treatment, as a function of the drug concentration for (A) HMC and (B) Vero cells. Cultured mammalian cells were infected with *T. cruzi* and incubated at 37 °C with Ris at indicated concentrations for 96 h. Experiments were carried out in quadruplicate and each bar represents one standard deviation.

groups has shown that *T. cruzi* mitochondrial membranes, in contrast to those of vertebrate cells, are rich in endogenous parasite sterols, which are thought to be required for their energy transducing activities [44]. Mitochondrial swelling was among the most prominent ultrastructural alterations seen in both epimastigotes and amastigotes treated with Ris (Fig. 3), consistent with the hypothesis that sterol depletion is one of the primary effects of this drug on the parasite. However, other ultrastructural effects were also observed for this drug, and could also be important in growth inhibition. For example, the early effects of Ris on the reservosomes, which are involved in endocytosis, storage and breakdown of nutrients [36,45], could hamper the proliferation process in epimastigotes. Although the precise molecular mechanisms of these effects are doubtless complex and at this time remain obscure, they could be related to altered protein synthesis and sorting associated with abnormal cell signalling, due to a depletion of essential poly-isoprenoids. Since Ris inhibits sterol biosynthesis (see above and ref. [16]), the accumulation of lipid droplets in the reservosomes could be a response of the parasite to the drug, as a consequence of the accumulation of abnormal lipids and/or the uptake of lipids from the culture medium. Other abnormalities such as cytoplasmic lipid inclusions and autophagic vacuoles, have also been noted in this and other trypanosomatid parasites treated with sterol biosynthesis inhibitors and are likely due to the accumulation of abnormal lipids and lipid precursors in these cells [38–43].

Although the primary target of Ris and other NBPs, FPPS, is an essential enzyme in all eukaryotic cells, the

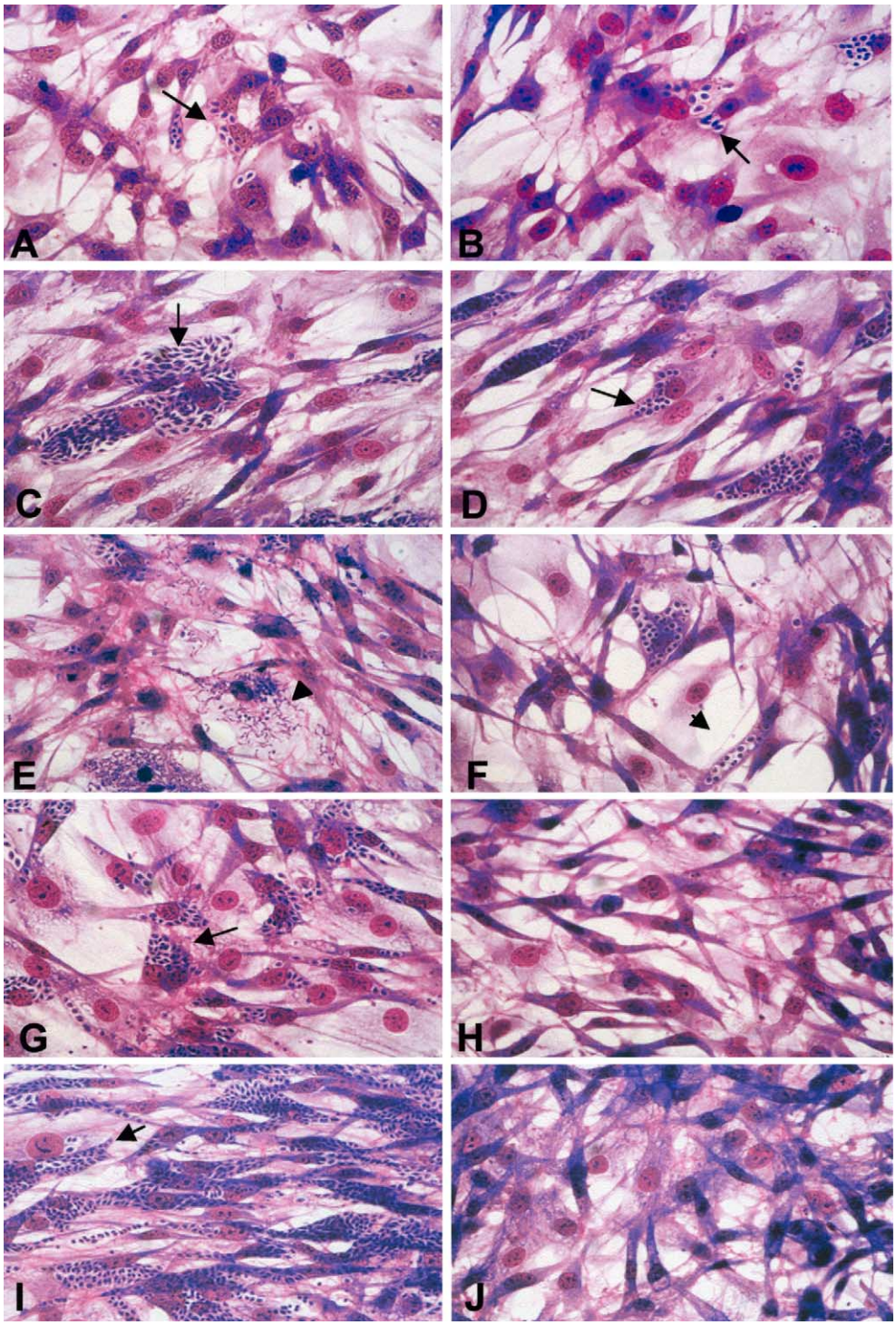

Fig. 6. Effects of risedronate on the morphology of HMC and intracellular *T. cruzi* (Y strain) stages. (A, C, E, G, I) untreated infected cultures. After 48 h of infection, large numbers of proliferating amastigotes were seen (arrow) (A). After 72 h of infection many oval-shaped parasites were seen and the amastigote-trypomastigote differentiation process began (C). After 96 h of infection the first parasite cycle inside the host cell was completed and the high number of intracellular trypomastigotes (arrow head) led to disruption of HMC (E), and infection of other host cells (arrows in G, I; 120 and 144 h after infection). (B, D, F, H, J) Infected cultures treated with 100 μM Ris immediately after the initial 2 h infection step. No apparent effects on amastigotes were seen after 48 h of treatment (arrow) (B). After 72 h (D) and 96 h (E) of infection, a progressive alteration of the parasites' shape was observed as well as a marked inhibition of the differentiation to trypomastigotes (F). Intracellular parasites were rarely detected after 120 or 144 h of treatment, while the host cells recover their normal morphology (H, J). Magnification: 1200×.

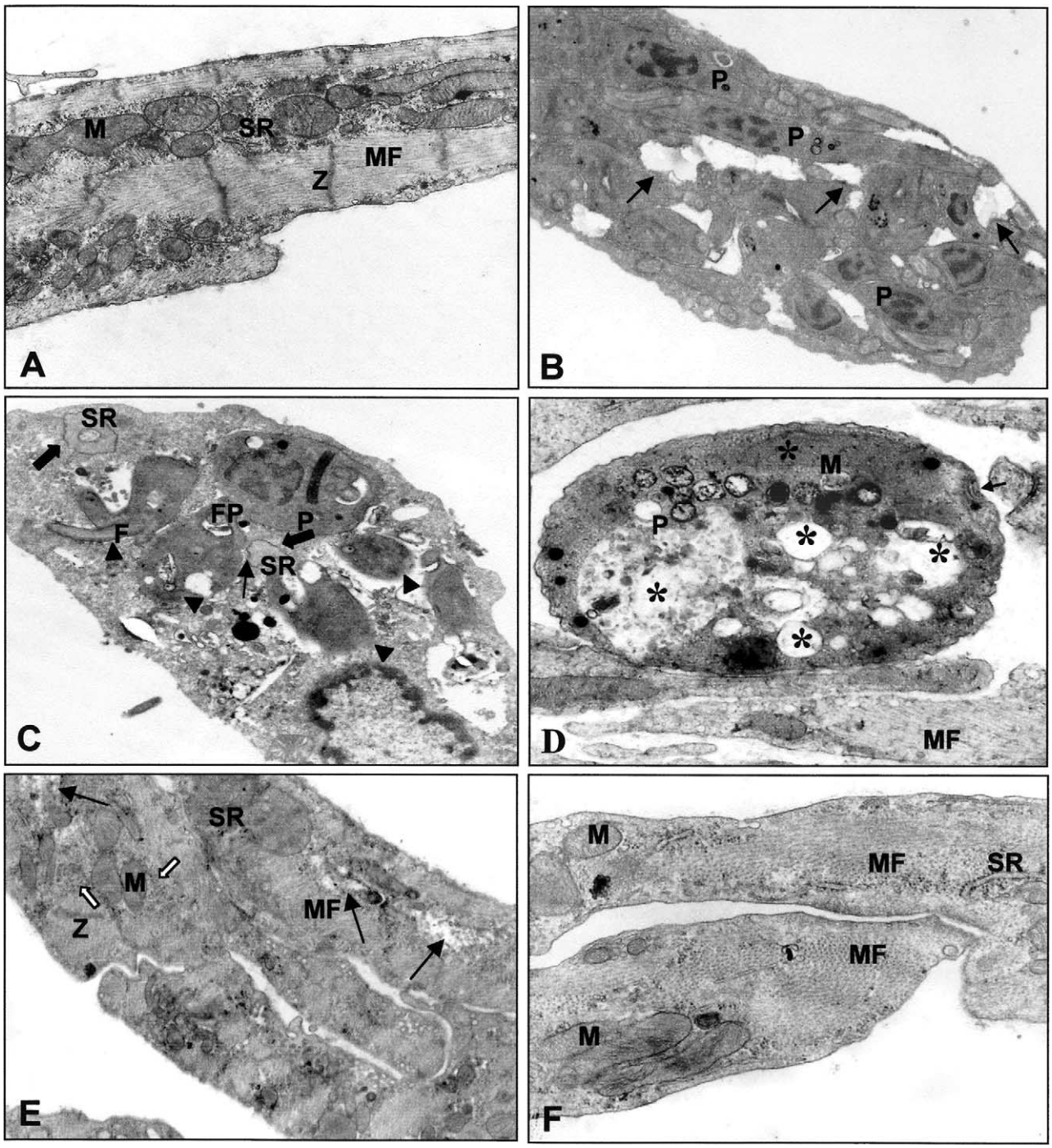

Fig. 7. Effects of risedronate on the ultrastructure of HMC and intracellular *T. cruzi* (Y strain) stages (A) non-infected and untreated HMC presenting myofibrils (MF) with normal Z line (Z), mitochondria (M), sarcoplasmic reticulum profiles (SR) and membrane invaginations. (B) Untreated HMC after 144 h of infection with *T. cruzi*, presenting several empty spaces (arrows) in the sarcoplasma close to internal parasites (P). (C) Infected HMC (144 h) treated with 100 μM Ris for 96 h, showed swelling of sarcoplasmic reticulum (large arrows) and bearing some damaged amastigotes (arrow heads). (D) Infected HMC (144 h) treated with 100 μM Ris for 96 h showing a parasite in detail with several alterations, such as mitochondrial swelling (white asterisk), altered flagellar pocket (small arrow), strong vacuolisation (asterisks). (E, F) Infected HMC (192 h) treated with 100 μM Ris for 144 h: HMC showed normal characteristics of the myofibrils, mitochondria, sarcoplasmic reticulum and ribosomes (white arrows); some regions of the sarcoplasma showed some electrondensity, suggesting recovery of the host cell biosynthetic machinery (arrows). Magnifications: (A) 8000×; (B) 10,000×; (C) 8000×; (D) 27,500×; (E) 11,429×; (F) 26,000×.

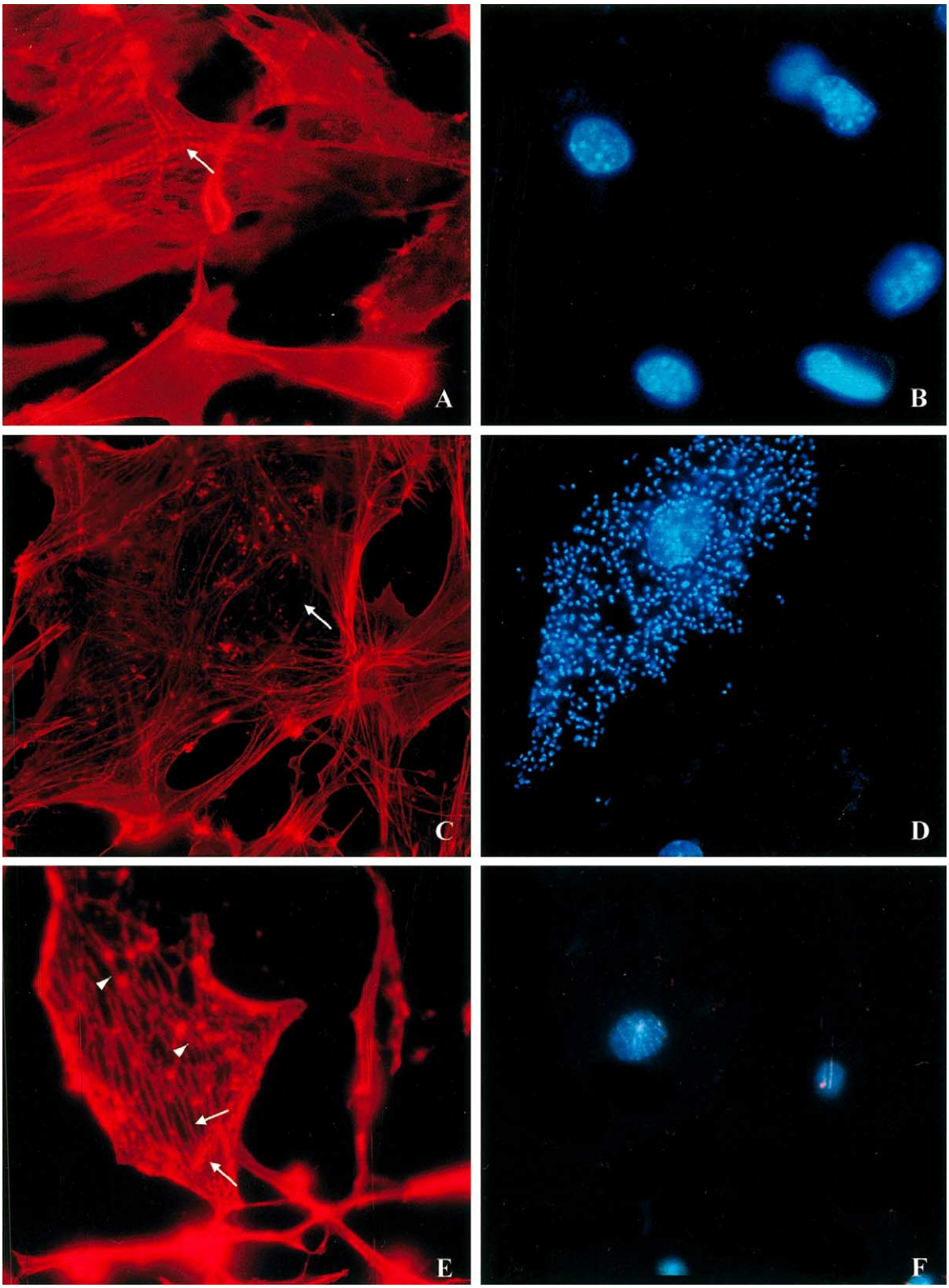

Fig. 8. Effect of risedronate on organization of actin cytoskeletal in *T. cruzi*-infected HMC. Infected HMC untreated and treated with Ris were double labelled with rhodamine–phalloidin and DAPI. Uninfected cells displayed well-developed myofibrils (arrow) (A) and nuclei stained with DAPI (B). HMC infected with trypomastigotes after 144 h showed broken myofibrils localized close to the parasites (small arrow) (C) and DAPI stained the host cells nucleus and the nucleus and kinetoplast of the parasites (D). Infected HMC treated with 100 μM Ris for 142 h (144 h of infection) presented polygonal (arrow head) as well as filamentous configuration of actin filaments (arrow) (E) and DAPI stained only the host cells nucleus, with no detectable intracellular parasites (D). Magnification: 1400×.

selective activity of bisphosphonates as anti-resorptive agents in mammals is thought to be due to their differential accumulation in the osteoclasts of bone [46,47]. Likewise, it has been argued that the selective anti-trypanosomatid and anti-apicomplexan activities of these compounds could be explained, at least in part, by their selective accumulation in the parasite due in part to the presence of acidocalcisomes, which are very rich in short-chain polyphosphates [14,15,48]. This hypothesis has recently received support from studies which demonstrate the accumulation of [^{3}H]-labelled pamidronate in intact acidocalcisomes of *T. cruzi* (Ruiz FA and Docampo R, unpublished results). In this work, we have investigated the molecular and cellular basis of the selective activity of Ris against the intracellular amastigote stage of the parasite by using both biochemical and ultrastructural techniques (Figs. 6–8). Our results show that, in contrast to the effects seen on parasite sterol content (Table 1), no effects of Ris were observed on the lipid composition of the host cells. At the ultrastructural level, our results show that in infected HMC cells treated with Ris, drug-induced damage is confined to the intracellular parasites, with the host cells being able to fully recover normal morphology, intracellular organization and contractility, at therapeutic doses (Figs. 7 and 8). It was previously shown by one of our groups (M.N.M.) that infection by *T. cruzi* induces a cytoskeletal disruption in HMCs, due to myofibrillar breakdown [35]. The present results confirm these effects of infection on actin filaments (Fig. 8C), and show that on treatment with Ris, reorganization of the actin-containing myofibrils to their normal state occurs via a characteristic polygonal arrangement (Fig. 8E). Lin et al. [49] have also recently described this polygonal configuration in dissociated cardiac myocytes as an indicator of myofibrillar reassembly. The polygonal configuration of actin-containing myofibrils was not observed in non-infected HMC treated with Ris (data not shown), indicating that this state is not directly due to drug treatment.

In conclusion, the results of the present study demonstrate rapid and drastic biochemical and ultrastructural effects of Ris on *T. cruzi* epimastigotes and amastigotes, effects not observed in the host cells. The action of the drug on both the extracellular and intracellular parasites leads to cell lysis 96–120 h after treatment (Figs. 1 and 3), an observation which suggests the potential for trypanocidal activity in vivo. This has been confirmed by the results of studies of a murine model of acute Chagas' disease ([50] accompanying article). Risedronate and related NBPs, are therefore interesting lead anti-*T. cruzi* compounds which could be further developed as novel chemotherapeutic agents for the treatment of Chagas' disease.

Acknowledgements

We are grateful to Dr. Maurílio, J. Soares for the critical reading of this manuscript, Dr. Andrea Henriques-Pons and Ricardo M. Santa-Rita for the support on the flow cytometry analysis, to Bernardo Visentin for his excellent technical assistance. This work was supported with grants from FIOCRUZ, CNPq and FAPERJ, and the Howard Hughes Medical Institute (Grant 55000620 to J.U.) and in part by the US Public Health Service (NIH grant GM 65307 to E.O. and R.D.; NIH NRSA grant GM 65782 to G.A.M.) and by the American Heart Association, Midwest Affiliate (E.O.) and National Center (R.D.).

References

[1] World Health Organisation. Control of Chagas disease. Tech Rep Ser 905;2002:1–109.
[2] Dias JCP. Epidemiologia. In: Brener Z, Andrade Z, Barral-Netto C, editors. *Trypanosoma cruzi* e doença de Chagas. Rio de Janeiro: Guanabara Koogan; 1999. p. 48–74.
[3] Urbina JA. Chemotherapy of Chagas disease. Curr Pharma Des 2002;8:287–95.
[4] Coura JR, De Castro SL. A critical review on Chagas disease chemotherapy. Memórias do Instituto Oswaldo Cruz 2002;97:3–24.
[5] Docampo R. Recent developments in the chemotherapy of Chagas disease. Curr Pharma Des 2001;7:1157–64.
[6] Rodriguez JB. Specific molecular targets to control tropical diseases. Curr Pharma Des 2001;7:1105–16.
[7] Martin MB, Arnold W, Heath III HT, Urbina JA, Oldfield E. Nitrogen-containing bisphosphonates as carbocation transition state analogs for isoprenoid biosynthesis. Biochem Biophys Res Commun 1999;263:754–8.
[8] Bergstrom J, Bostedor DRG, Massarachia PJ, Reszka AA, Rodan GA. Alendronate is a specific, nanomolar inhibitor of farnesyl diphosphate synthase. Arch Biochem Biophys 2000;373:231–41.
[9] Cromartie TH, Fisher KJ, Grossman JN. The discovery of a novel site of action for herbicidal bisphosphonates. Pest Biochem Physiol 1999;63:114–26.
[10] Grove JE, Brown RJ, Watts DJ. The intracellular target of the antiresorptive aminobisphosphonate drugs in *Dictyostelium discoideum* is the enzyme farnesyl diphosphate synthase. J Bone Mineral Res 2000;15:971–81.
[11] van Beek E, Pieterman E, Cohen L, Löwik C, Papapoulos S. Nitrogen-containing bisphosphonates inhibit isopentenyl pyrophosphate isomerase/farnesyl pyrophosphate synthase activity with relative potencies corresponding to their anti-resorptive potencies in vitro and in vivo. Biochem Biophys Res Commun 1999a;251:491–4.
[12] van Beek E, Pieterman E, Cohen L, Löwik C, Papapoulos S. Farnesyl pyrophosphate synthase is the molecular target of nitrogen-containing bisphosphonates. Biochem Biophys Res Commun 1999;264:108–11.
[13] Montalvetti A, Bailey BN, Martin MB, Severin GW, Oldfield E, Docampo R. Bisphosphonates are potent inhibitors of *Trypanosoma cruzi* farnesyl pyrophosphate synthase. J Biol Chem 2001;276:33930–7.
[14] Docampo R, Moreno SNJ. The acidocalcisome. Mol Biochem Parasitol 2001;33:151–9.
[15] Docampo R, Moreno SNJ. Bisphosphonates as chemotherapeutic agents against trypanosomatids and Apicomplexan parasites. Curr Drug Targets-Infect Dis 2001;1:51–61.
[16] Martin MB, Grimley JS, Lewis JC, Heath III HT, Bailey BN, Kendrick H, et al. Bisphosphonates inhibit the growth of *Trypanosoma brucei*, *Trypanosoma cruzi*, *Leishmania donovani*, *Toxoplasma gondii* and *Plasmodium falciparum*: a potential route to chemotherapy. J Med Chem 2001;44:909–16.
[17] Martin MB, Sanders JM, Kendrick H, de Luca-Fradley K, Lewis JC, Grimley JS, et al. Activity of bisphosphonates against *Trypanosoma brucei rhodesiense*. J Med Chem 2002;45:2904–14.

[18] Rodriguez N, Bailey BN, Martin MB, Oldfield E, Urbina JA, Docampo R. Radical cure of experimental cutaneous leishmaniasis by the bisphosphonate pamidronate. J Infect Dis 2002;186:138–40.
[19] Szajnman SH, Bailey BN, Docampo R, Rodríguez JB. Bisphosphonates derived from fatty acids are potent growth inhibitors of *Trypanosoma cruzi*. Bioorg Med Chem Lett 2001;11:789–92.
[20] Yardley V, Khan A, Martin MB, Slifer TR, Araujo FG, Moreno SNJ, et al. In vivo activities of farnesyl pyrophosphate synthase inhibitors against *Leishmania donovani* and *Toxoplasma gondii*. Antimicrob Agents Chemother 2002;46:929–31.
[21] Crandall C. Risedronate: a clinical review. Arch Intern Med 2001;161:353–60.
[22] Silva LHP, Nussenszweig V. Sobre uma cepa de *Trypanosoma cruzi* virulenta para o camundongo branco. Folia Clinica Biologica 1953;20:191–207.
[23] De Maio A, Urbina JA. *Trypanosoma* (*Schizotrypanum*) *cruzi*: terminal oxidases in exponential and stationary growth phase epimastigotes cultured in vitro. Acta Cientifica Venezolana 1984;35:136–41.
[24] Hudson L, Grover F, Gutteridge WE, Klein RA, Peters W, Neal RA, et al. Suggested guidelines for work with live *Trypanosoma cruzi*. Trans R Soc Trop Med Hyg 1983;77:416–9.
[25] Meirelles MN, Araújo-Jorge TC, Miranda CF, DeSouza W, Barbosa HS. Interaction of *Trypanosoma cruzi* with heart muscle cells: Ultrastructural and cytochemical analysis of endocytic vacuole formation and effect upon myogenesis in vitro. Eur J Cell Biol 1986;41:198–206.
[26] Urbina JA, Lazardi K, Aguirre T, Piras MM, Piras R. Antiproliferative synergism of the allylamine SF 86-327 and ketoconazole on epimastigotes and amastigotes of *Trypanosoma* (*Schizotrypanum*) *cruzi*. Antimicrob Agents Chemother 1988;32:1237–42.
[27] De Castro SL, Soeiro MN, Meirelles MNL. Trypanosoma cruzi: effect of phenothiazines on the parasite and its interaction with host cells. Memórias do Instituto Oswaldo Cruz 1992;87:209–15.
[28] Liendo A, Lazardi K, Urbina JA. In vitro antiproliferative effects and mechanism of action of the bis-triazole D0870 and its S(-) enantiomer against *Trypanosoma cruzi*. J Antimicrob Chemother 1998;41:197–205.
[29] Liendo A, Visbal G, Piras MM, Piras R, Urbina JA. Sterol composition and biosynthesis in *Trypanosoma cruzi* amastigotes. Mol Biochem Parasitol 1999;104:81–91.
[30] Urbina JA, Payares G, Molina J. Cure of short- and long-term experimental Chagas disease using D0870. Science 1996;273:969–71.
[31] Urbina JA, Payares G, Contreras LM, Liendo A, Sanoja C, Molina J, et al. Antiproliferative effects and mechanism of action of SCH 56592 against *Trypanosoma* (*Schizotrypanum*) *cruzi*: In vitro and in vivo studies. Antimicrob Agents Chemother 1998;42:1771–7.
[32] Contreras LM, Vivas J, Urbina JA. Altered lipid composition and enzyme activities of plasma membranes from *Trypanosoma* (*Schizotrypanum*) *cruzi* epimastigotes grown in the presence of sterol biosynthesis inhibitors. Biochem Pharmacol 1997;53:697–704.
[33] Cuzner ML, Davison AN. Quantitative thin layer chromatography of lipids. J Chromatogr 1967;27:388–97.
[34] Ames B, Dubin D. The role of polyamines in the neutralization of deoxyribonucleic acid. J Biol Chem 1960;235:769–75.
[35] Pereira MCS, Costa M, Chagas Filho C, Meirelles MNL. Myofibrillar breakdown and cytoskeletal alterations in heart muscle cells during invasion by *Trypanosoma cruzi:* immunological and ultrastructural study. J Submicrosc Cytol Pathol 1993;25:559–69.
[36] Soares MJ. The reservosome of *Trypanosoma cruzi* epimastigotes: an organelle of the endocytic pathway with a role on metacyclogenesis. Memórias do Instituto Oswaldo Cruz 1999;94:139–41.
[37] Santa-Rita RM, Menna-Barreto RFS, De Castro SL. Studies with analogues of phospholipids against *Trypanosoma cruzi* and *Leishmania amazonensis.* In: Program and Abstracts of the Fifth COST-B9 Congress on Antiprotozoal Chemotherapy, London, 2002 [Abstract 25].
[38] Docampo R, Moreno SNJ, Turrens JF, Katzin AM, Gonzales-Cappa SM, Stoppani AOM, et al. Biochemical and ultrastructural alterations produced by miconazole and ketoconazole in *Trypanosoma cruzi*. Mol Biochem Parasitol 1981;3:169–80.
[39] Lazardi K, Urbina JA, DeSouza W. Ultrastructural alterations induced by two ergosterol biosynthesis inhibitors, ketoconazole and terbinafine, on epimastigotes and amastigotes of *Trypanosoma* (*Schizotrypanum*) *cruzi*. Antimicrob Agents Chemother 1990;34:2097–105.
[40] Lazardi K, Urbina JA, DeSouza W. Ultrastructural alterations induced by ICI 195,739, a bis triazole with strong antiproliferative action against *Trypanosoma* (*Schizotrypanum*) *cruzi*. Antimicrob Agents Chemother 1991;35:736–40.
[41] Rodrigues JCP, Attias M, Rodriguez C, Urbina JA, DeSouza W. Ultrastructural and biochemical alterations induced by 22,26-azasterol, a $\Delta^{24(25)}$ sterol methyl transferase inhibitor, on promastigote and amastigote forms of *Leishmania amazonensis*. Antimicrob Agents Chemother 2002;46:487–99.
[42] Vannier-Santos MA, Urbina JA, Martiny A, Neves A, DeSouza W. Alterations induced by the antifungal compounds ketoconazole and terbinafine in *Leishmania*. J Eukaryotic Microbiol 1995;42:337–46.
[43] Vivas J, Urbina JA, DeSouza W. Ultrastructural alterations in *Trypanosoma* (*Schizotrypanum*) *cruzi* induced by $\Delta^{24(25)}$ sterol methyl transferase inhibitors and their combinations with ketoconazole. Int J Antimicrob Agents 1996;7:235–40.
[44] Rodrigues CO, Catisti R, Uyemura SA, Vercesi AE, Lira R, Rodriguez C, et al. The sterol composition of *Trypanosoma cruzi* changes after growth in different culture media and results in different sensitivity to digitonin-permeabilization. J Eukaryot Microbiol 2001;48:588–94.
[45] Engel JC, Doyle PS, Palmer J, Hsieh I, McKerrow JH. Cysteine protease inhibitors alter Golgi complex ultrastructure and function in *Trypanosoma cruzi*. J Cell Sci 1998;111:597–606.
[46] Rodan GA. Mechanisms of action of bisphosphonates. Annu Rev Pharmacol Toxicol 1998;38:375–88.
[47] Rodan GA, Martin TJ. Therapeutic approaches to bone diseases. Science 2000;289:1508–14.
[48] Urbina JA, Moreno B, Vierkotter S, Oldfield E, Payares G, Sanoja C, et al. *Trypanosoma cruzi* contains major pyrophosphate stores, and its growth in vitro and in vivo is blocked by pyrophosphate analogues. J Biol Chem 1999;274:33609–15.
[49] Lin ZX, Holtzer S, Schultheiss T, Murray J, Masaki T, Fischman DA, et al. Polygons and adhesion plaques and disassembly and assembly of myofibrils in cardiac myocytes. J Cell Biol 1989;108:2355–67.
[50] Garzoni LR, Caldera A, Meirelles MNL, de Castro SL, Docampo R, Meints GA, et al. Antiparasitic activity of risedronate in a murine model of acute Chagas disease. Int J Antimicrob Agents 2004;23:286–90.